

3-1-2020

## Static Characteristics of 7/24 Taper Connection.

Hazem El-Shourbagy

*Assistant Professor of Production Engineering Department, Faculty of Engineering, Mansoura University, Mansoura, Egypt.*

Follow this and additional works at: <https://mej.researchcommons.org/home>

---

### Recommended Citation

El-Shourbagy, Hazem (2020) "Static Characteristics of 7/24 Taper Connection.," *Mansoura Engineering Journal*: Vol. 19 : Iss. 1 , Article 16.

Available at: <https://doi.org/10.21608/bfemu.2021.163350>

This Original Study is brought to you for free and open access by Mansoura Engineering Journal. It has been accepted for inclusion in Mansoura Engineering Journal by an authorized editor of Mansoura Engineering Journal. For more information, please contact [mej@mans.edu.eg](mailto:mej@mans.edu.eg).

## STATIC CHARACTERISTICS OF 7/24 TAPER CONNECTION

BY

S. HAZEM

Dept. of Production Engineering, Faculty of Engineering,  
Mansoura University, Mansoura, EGYPT.

### الخصائص الاستاتيكية للوصلة المسلوقة ذات النسبة ٧/٢٤

ملخص: هذا البحث يقوم من خلال التحليل النظري بطريقة الجزئيات المحددة على استنباط الخواص الاستاتيكية الأساسية للوصلات المسلوقة ذات النسبة ٧/٢٤ ممثلة في جسيمااتها، إجهادات القص، إجهادات الضغط والنتيجة من تأثير قوى الثني الخارجية. كذلك استنباط العلاقات التي تربط بين الأبعاد الرئيسية لهذه التوعية من الوصلات المسلوقة.

**ABSTRACT:** The current international standards of taper connections of ratio 7/24 have several dimensional specifications, even for the same size of such tapers. The present work investigates theoretically, by means of the Finite Element Analysis, the basic static characteristics of such connection in form of its stiffness, shear and compression stresses that caused by external bending load. Also, it deduces the interrelation between the main dimensions of such a taper connection.

### INTRODUCTION:

The nose of a machine tool spindle is generally bored out to receive and locate tools or tool-holders. The main advantages of taper location, with no poor centering, involve ensuring concentricity with the spindle journals, and eliminating all plays. The taper connections may be grouped into two main groups; the self-holding group, e.g. Morse tapers, and self-releasing group, e.g. taper connection of ratio 7/24.

Because of the widespread international use of taper connections, the original Morse and the 7/24 tapers, provide the bases of the current international metric standards. At present the 7/24 taper connections play the kernel function as automatic tool changing (ATC) system for the advanced machine tools, which are widely employed in metal work industries.

Several research works [1-8] on the 7/24 taper connections have been published. Through these works, the influences of tool-shank taper errors, tool centering, mounting and releasing forces [1,6], static bending stiffness [2-4 and 7], torsional stiffness [3], taper inclination angle and axial displacement [4], contact stiffness [6], static and dynamic behaviours [7,8] have been clarified to a great extent. During these works, however, different standards of such tapers have been used, such as the GOST [1-3], JIS [4], JIS and ISO [6,7].

In this paper, therefore, the 7/24 taper No.30 has been investigated theoretically, by means of the Finite Element Analysis, to clarify the basic static characteristics, from which the main dimensions of such joint type may be considered.

## BASIC CONCEPTS OF 7/24 TAPERS:

A 7/24 taper connection consists of a bored spindle nose and tapered tool shank, as shown in Fig.1. The main standard specifications according to the ISO/TC 39-726-1972 and the JIS/B6101-1982 of such tapers are shown in Table 1. From which, it is clear that both the values of the taper gauge diameter ( $d$ ) and the spindle nose height ( $L$ ), are same for the two concerned standards, however the spindle nose diameter ( $D$ ) has different and inconsistent values between these two standards.

In addition, some scale factors  $n$ ,  $l$ , and  $m$  have been deduced, as shown in Table 2. These scale factors are namely,  $[n=d(BT..)/d(BT30)]$  as the taper gauge diameter scale factor,  $[l=L(BT..)/L(BT30)]$  as the spindle nose height scale factor, and  $[m=D(BT..)/D(BT30)]$  as the spindle nose diameter scale factor. These scale factors have been plotted, as shown in Figs. (2-4), from which a clear straightline relationships have been observed. However, careful investigation should be considered to Fig.4, as the ISO standard starts with spindle nose diameter of taper No.BT40, while it is with BT30 for the JIS ones.

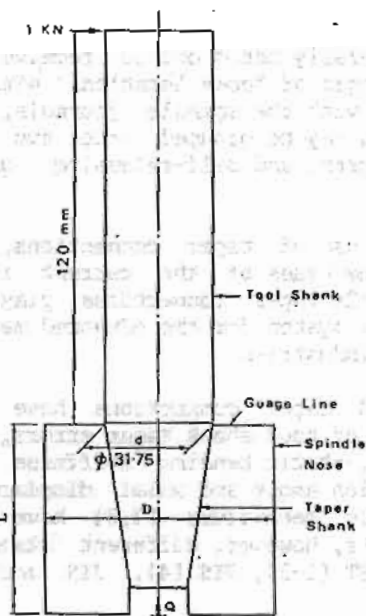


Fig.1 7/24 Taper connection geometry.

Table 1 Main Standard Specifications of Taper Connections

|   |     | BT30   | BT35   | BT40   | BT45   | BT50    | BT55    | BT60    |
|---|-----|--------|--------|--------|--------|---------|---------|---------|
| d | JIS | 31.750 | 38.100 | 44.450 | 57.150 | 69.850  | 88.900  | 107.950 |
|   | ISO | 31.750 | 38.100 | 44.450 | 57.150 | 69.850  | 88.900  | 107.950 |
| D | JIS | 69.832 | 79.357 | 88.882 | 101.60 | 128.570 | 152.400 | 221.440 |
|   | ISO | --     | --     | 62-85  | 100    | 100-180 | 155,180 | 205-300 |
| L | JIS | 73     | 86     | 100    | 120    | 140     | 170     | 220     |
|   | ISO | --     | --     | 100    | 120    | 140     | 170     | 220     |

Table 2 dimensionless Scale Factors

|   |     | BT30 | BT35  | BT40        | BT45  | BT50        | BT55        | BT60        |
|---|-----|------|-------|-------------|-------|-------------|-------------|-------------|
| n | JIS | 1.0  | 1.2   | 1.4         | 1.8   | 2.2         | 2.8         | 3.4         |
|   | ISO | --   | --    | 1.4         | 1.8   | 2.2         | 2.8         | 3.4         |
| l | JIS | 1.0  | 1.178 | 1.370       | 1.640 | 1.918       | 2.438       | 3.014       |
|   | ISO | --   | --    | 1.370       | 1.640 | 1.918       | 2.438       | 3.014       |
| m | JIS | 1.0  | 1.136 | 1.273       | 1.455 | 1.840       | 2.180       | 3.170       |
|   | ISO | --   | --    | 0.888-1.217 | 1.430 | 1.430-2.580 | 2.220-2.580 | 2.940-4.296 |



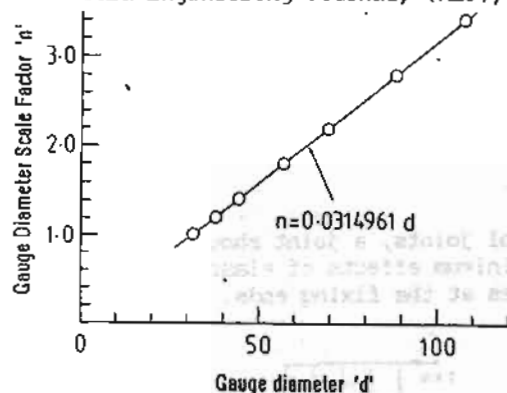


Fig.2 Relation between the scale factor factor 'n' and gauge diameters.

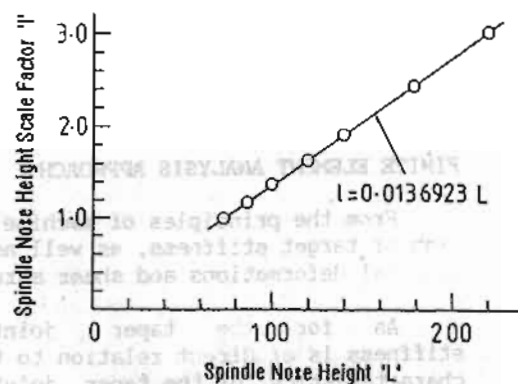


Fig.3 Relation between the scale factor 'l' and spindle nose heights.

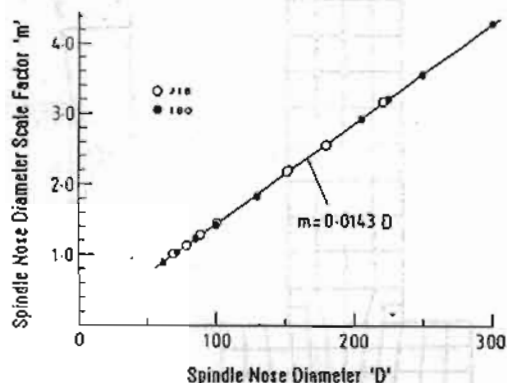


Fig.4 Relation between the scale factor 'm' and spindle nose diameters.

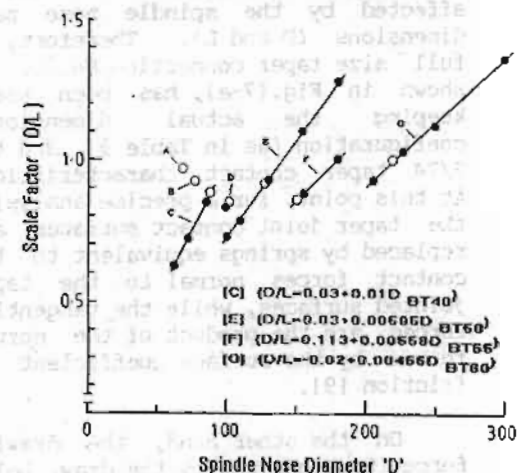


Fig.5 Relation between the scale factor 'D/L' and spindle nose diameters.

From the obtained information, some more relations have been observed between a scale factor of the ratio (D/L) against the spindle nose diameter, however these relations are related according to a concerned taper size, as shown in Fig.5. Similarly non-linear relations have been also observed between another scale factor (d/D) against the spindle nose diameter, as shown in Fig.6.

From above, it is clear that there are no close or clear relationships between the main dimensions (d, D, and L) of one taper size, while (as shown in Table 2) there are clear relationships between

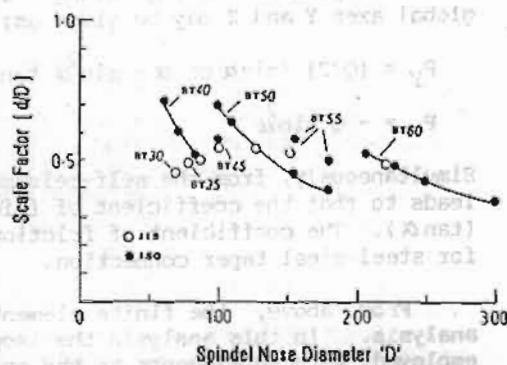


Fig.6 Relation between the scale factor 'd/D' and spindle nose diameters.

each of the main dimensions and the corresponding ones of other taper sizes.

#### FINITE ELEMENT ANALYSIS APPROACH:

From the principles of machine tool joints, a joint should be designed with high or target stiffness, as well as minimum effects of elastic deformations due to local deformations and shear stresses at the fixing ends.

As for the taper joints, stiffness is of direct relation to the characteristics of the taper jointed portion, however local deformations and shear stresses are directly affected by the spindle nose main dimensions (D and L). Therefore, a full size taper connection No.30, as shown in Fig.(7-a), has been used, keeping the actual dimensional configuration (as in Table 1), and the 7/24 taper contact characteristics. At this point, for a precise analysis, the taper joint contact surfaces are replaced by springs equivalent to the contact forces normal to the taper jointed surfaces, while the tangential forces are the product of the normal forces by the surface coefficient of friction [9].

On the other hand, the drawing force (Q) subjected by the draw bolt, should also be transmitted to the jointed surfaces, as shown in Fig.(7-b). From which the analysis of the force components acting along the global axes Y and Z may be given as;

$$P_y = (Q/2) (\sin\alpha \cos\alpha - \sin^2\alpha \tan\alpha)$$

$$P_z = -Q \sin^2\alpha$$

Simultaneously, from the self-release nature of the 7/24 taper connection, this leads to that the coefficient of friction ( $\mu$ ) at the jointed portion is equal to ( $\tan\alpha$ ). The coefficient of friction has been, therefore, taken equal to 0.146 for steel-steel taper connection.

From above, the finite element has been carried out in two-dimensional analysis. In this analysis the isoparametric four-nodes element type has been employed, with 60 elements to the spindle nose model, 42 elements for the taper shank model, and 52 elements to the tool shank model. During this analysis the

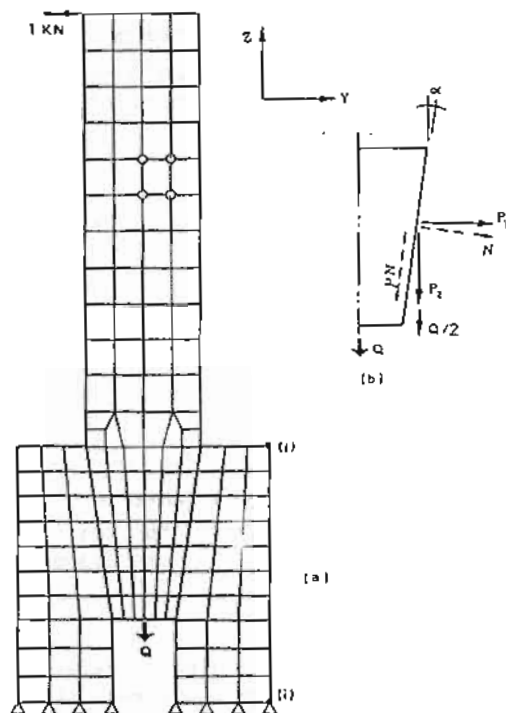


Fig.7 Mesh model of 7/24 taper No.30.

spindle nose diameter ( $D$ ) and the spindle nose height ( $L$ ) have been varied, while the same gauge diameter of taper No.30 is employed. Thus the effects of the dimensionless scale factors ' $I$ ' as the ratio of the spindle nose diameter to the gauge diameter ( $D/d$ ), and ' $J$ ' as the ratio of the spindle nose height to the gauge diameter ( $L/d$ ), have been investigated to clarify the bending stiffness measured at the point of the external load, as well as the local deformations, shear and compression stresses at the fixing ends due to the external loading.

## RESULTS & DISCUSSION:

Through the theoretical analysis, the bending stiffness at the loading point, compression stresses in Y and Z-directions, and the shear stresses at the fixing ends have been calculated.

The effects of the scale factors ' $I$ ' and ' $J$ ' on the bending stiffness, are shown in Fig.8. From this figure it is clear that, for a given taper gauge diameter, the bending stiffness increases dramatically with the increase of the scale factor ' $I$ ', while it is inversely proportional to the scale factor ' $J$ '. By another words, the bending stiffness increases with increasing the spindle nose diameter ( $D$ ) and decreasing the spindle nose height ( $L$ ). In addition, the rate of change of the bending stiffness decreases at small values of the scale factor ' $J$ '. Therefore, according to the required or the target bending stiffness, of the objective system, the suitable nose diameter(s) as well as the spindle nose height(s) may be obtained.

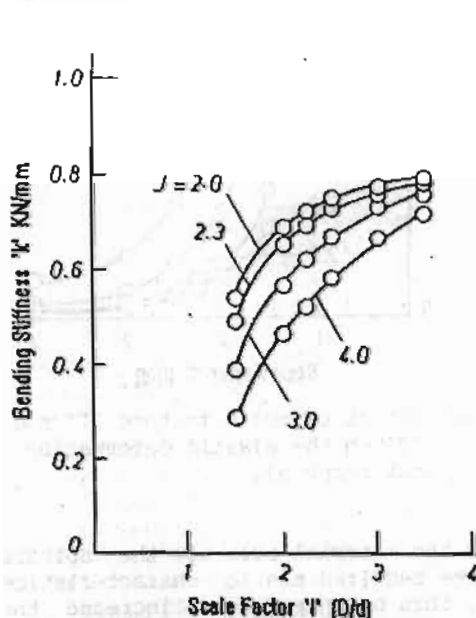


Fig.8 Effect of scale factors ' $I$ ' and ' $J$ ' on the bending stiffness.

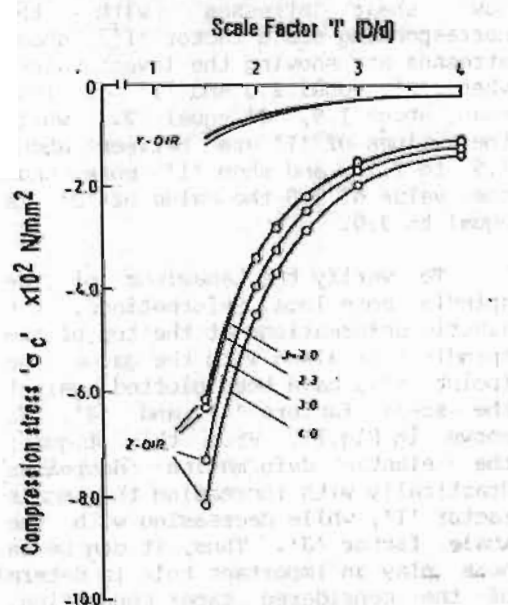


Fig.9 Effect of scale factors ' $I$ ' and ' $J$ ' on the compression stresses.



In this regard, it is expected from above to have several values of the spindle nose diameters and the corresponding heights. The resultant local deformations, shear and compression stresses, therefore, would be another factors to be considered. From the theoretical analysis, it has been found that the compression and shear stresses are with high values at the fixing end 'i' (as shown in Fig.7). The obtained resultant compression stresses in the Y and Z-directions, are shown in Fig.9, from which it can be said that the compression stresses in the Z-direction are dominating the elastic deformations of the spindle nose. It is decreasing with increasing the scale factor 'I' and decreasing with the scale factor 'J'. Also, the shear stresses at the same point 'i' are showing a similar trend, as shown in Fig.10, however with more flat rate of change at the values of scale factor 'I' more than the value of about 2.0. Also, it is worthy to point out that the scale factor 'J' shows different low shear stresses with the corresponding scale factor 'I'; shear stresses are showing the lowest values when 'J' equal 2.0 and 'I' is less than about 1.9, 'J' equal 2.3 while the values of 'I' are between about 1.9 to 2.75, and when 'I' more than the value of 3.0 the value of 'J' is equal to 3.0.

To verify the behaviour of the spindle nose local deformations, the elastic deformations at the top of the spindle nose along with the gauge line (point 'j'), have been plotted against the scale factors 'I' and 'J', as shown in Fig.11. From this figure, the elastic deformation decreases drastically with increasing the scale factor 'I', while decreasing with the scale factor 'J'. Thus, it can be said that the material bulk of the spindle nose play an important role in determining the required static characteristics of the considered taper connection. Also, this bulk tends to increase the spindle nose diameter, while decreasing the spindle nose height, as a result to minimize the local deformations and shear stresses of the spindle nose.

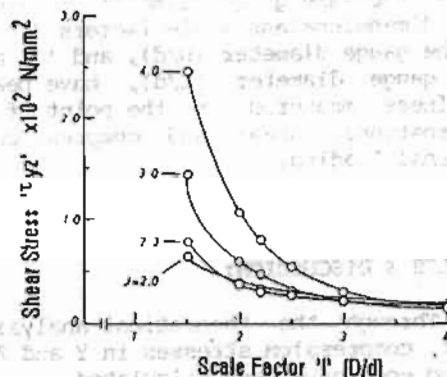


Fig.10 Effect of scale factors 'I' and 'J' on the shear stresses.

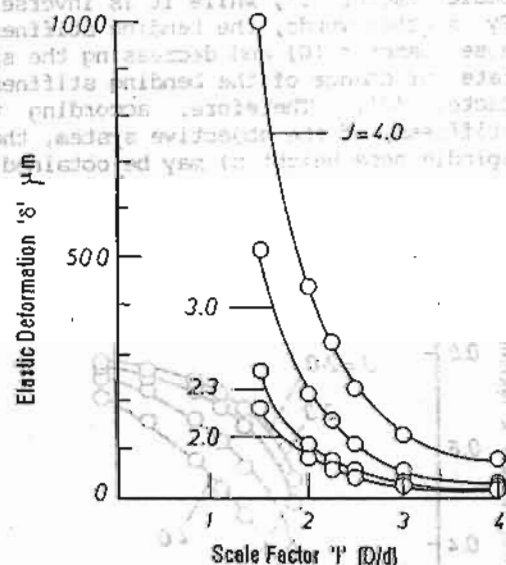
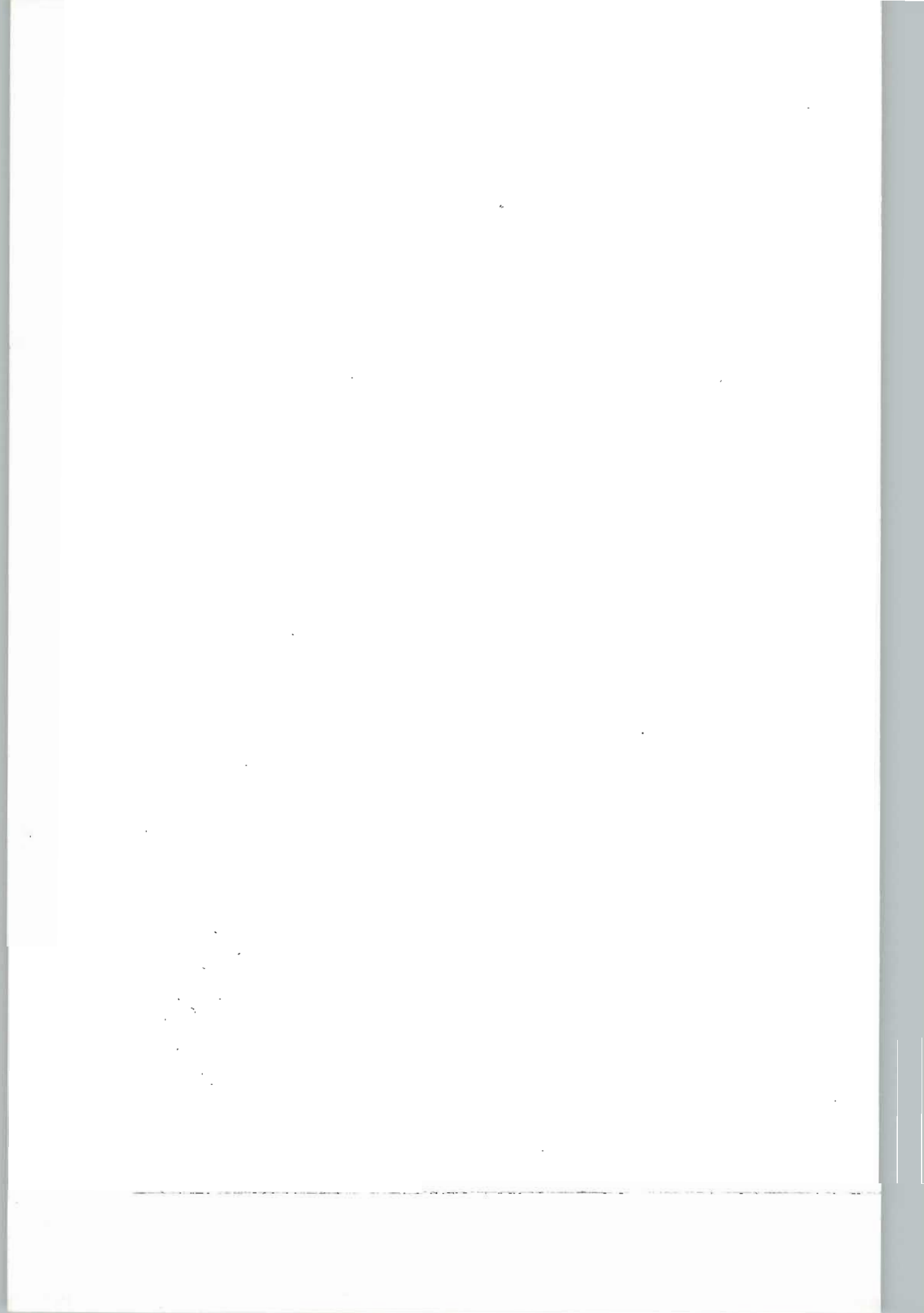


Fig.11 Effect of scale factors 'I' and 'J' on the elastic deformation (at point j).





## CONCLUDING REMARKS:

From the theoretical analysis, it can be envisaged that the required bending stiffness at the loading point, as well as the permissible shear and compression stresses at the fixing ends, are the main factors in determining the spindle nose main dimensions.

In addition, it is remarkable to point out that the largest the spindle nose diameter ( $D/d > [2.0 \cdot d(BT30)]$ ) and the spindle nose height ( $L/D < 1.0$ ), more reasonable the static characteristics that may be achieved. However, this achievement should be according to the concerned machine tool desired cutting accuracy.

## NOMENCLATURE:

|   |   |
|---|---|
| $d$ : Taper gauge diameter, mm;                                 | $D$ : Spindle nose diameter, mm;                    |
| $I$ : Ratio of the spindle nose diameter to the gauge diameter; |   |
| $J$ : Ratio of the spindle nose height to the gauge diameter;   |   |
| $K$ : Bending Stiffness, KN/mm;                                 | $l$ : Spindle nose height scale factor;             |
| $L$ : Spindle nose height, mm;                                  | $m$ : Spindle nose diameter scale factor;           |
| $n$ : Taper gauge diameter scale factor;                        | $Q$ : Drawing force, KN;                            |
| $\alpha$ : Taper angle, deg.;                                   | $\mu$ : Coefficient of friction;                    |
| $\delta$ : Elastic deformation, $\mu$ m;                        | $\tau_{yz}$ : Shear stress, N/mm <sup>2</sup> ; and |
| $\sigma_c$ : Compression stress, N/mm <sup>2</sup> ;            |   |

## REFERENCES:

- [1] Martynov A.D. and Sinelshchikova T.K., " Tolerances for Tool-Mounting Tapers ", Machines and Tooling, Vol.40, No.5, p.20, 1969.
- [2] Levina Z.M., " Stiffness Calculations for Cylindrical and Taper Joints" , Machines and tooling, Vol.41, No.3, p.51, 1970.
- [3] Levina Z.M., " Taper-Connexion Stiffness ", Machines and Tooling, Vol. 44, No.10, p.21, 1973.
- [4] Tsutsumi M. et al, " Static Characteristics of 7/24 Taper Joint for Machining Centers (1st Report, Effects of Taper Size and Angle Error)", Bulletin of the JSME, Vol.26, No.213, p.461, 1983.
- [5] Taniguchi A. et al, " Treatment of Contact Stiffness in Structural Analysis (1st Report, Mathematical Model of Contact Stiffness and its Applications ", Bulletin of the JSME, Vol.27, No.225, p.601, 1984.
- [6] Tsutsumi M. et al, " Study on the Characteristics of 7/24 Taper Joints ", Trans. of the JSME, Vol.51, No.462, p.425, 1985.[In Japanese]
- [7] Hazem S. et al, " A New Modular Tooling System of Curvic Coupling Type ", 26th Int. MTDR Conf., p.261, 1986.
- [8] Kim T.R., " Identification of Joint Parameters for a Taper Joint ", Trans. of the ASME, J. Eng. Ind., Vol.111, p.282, August 1989.
- [9] Rack N. et al, " Pressure Distribution and Deformations of Machined Components in Contact ", Int. J. Mech. Sci., Vol.15, p.993, 1973.